Approaches to Hysteresis of Transport Relations in Toroidal Plasmas[*]

Sanae-I. ITOH[1,2], Shigeru INAGAKI[1,2], Jiaqi DONG[3] and Kimitaka ITOH[2,4]

[1]*Research Institute for Applied Mechanics, Kyushu University, Kasuga 816-8580, Japan*
[2]*Research Center for Plasma Turbulence, Kyushu University, Kasuga 816-8580, Japan*
[3]*Southwestern Institute of Physics, PO Box 432, Chengdu, People's Republic of China*
[4]*National Institute for Fusion Science, Toki 509-5292, Japan*

In this overview, we explain methods to identify hysteresis in the gradient-flux relation for energy transport in a core plasma, which is revealed by a power modulation experiment. Two approaches to experimentally observe the hysteresis relation are discussed in detail. Advanced data analysis methods are also illustrated. A theoretical analysis of the process that couples heat to turbulence is also addressed.

1. Background and Introduction

There have been multiple experimental reports (e.g., W7-AS [1], D-III D [2], and LHD [3]) that the gradient-flux relation has hysteresis and that the heat flux may directly depend on the heating power (Fig. 1). This view contrasts with the conventional view of the plasma transport. In a conventional view, the heat flux is expressed in terms of the local plasma parameters and their gradients, e.g., [4, 5]. The influence of heating on transport is considered to appear through indirect influences of enhanced gradients or the generation of energetic particles. In the new picture of transport [1–3], the time scale for the response of the heat flux can be much faster than that of global plasma parameters such as temperature and temperature gradient or than that of building up energetic particles. The switching time (on/off) in the modulational electron cyclotron (EC) heating is shorter than a millisecond. The global plasma parameters change during this time, which is on the order of the energy confinement time (a few 10 s to a few 100 ms). The change in the heat flux is found to occur within the former shorter time, not with those for the global parameters [3, 6]. Therefore, the heat flux cannot be expressed as a single-valued function of the local global plasma parameters.

These reports may not have been considered seriously by the majority of experimentalists. One of the possible reasons (except human factors) is that the "heating power" was theoretically evaluated and was not independently measured. The possibility of an alternative interpretation that the heating power is completely different from the theoretical calculation (so that there is no hysteresis in
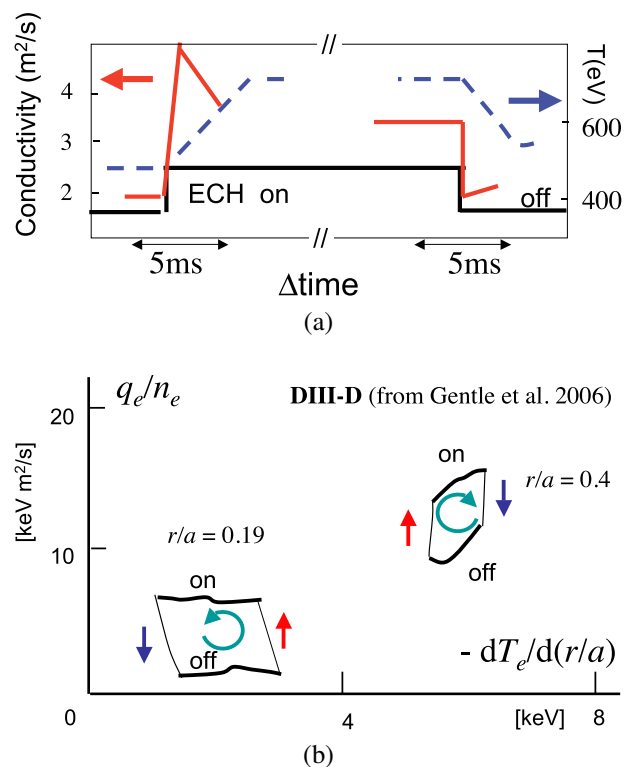

Fig. 1 Observations for (a) W7-AS (drawn based on Ref. [1]) and (b) D-III D (drawn based on Ref. [2]).

the gradient-flux relation) could not be completely refuted.

If hysteresis really exists and the heat flux directly depends on the heating power, then the discrepancy between the "power-balance" and "heat-pulse" conductivities [4] is naturally resolved. In addition, this hysteresis could have a profound impact on our evaluation of the dynamical re-

sponse of burning plasmas.

In this overview, we explain a method to identify the hysteresis in the gradient-flux relation for energy transport in a core plasma, which is revealed by the power modulation experiment. Our aim is to widely communicate the application of this advanced data analysis method.

2. Experimental Confirmation

To be decisive, the hysteresis in the gradient-flux relation and the gradient-fluctuation intensity relation was simultaneously measured while performing the modulational EC heating experiment (Fig. 2). The two were identified simultaneously [6, 7] to avoid the possibility that the error in the absorption power directed an erroneous hysteresis in the gradient-flux relation. If there is no hysteresis in the heat flux, the hysteresis in the gradient-fluctuation relation should not appear. Therefore, the hysteresis in the gradient-flux relation can be confirmed.

2.1 Experimental procedure

The essentials of the experimental procedure are illustrated here. A modulated electron cyclotron heating (MECH, also modulation ECH) experiment was performed in which a periodic on-off of the ECH power is imposed on a low density plasma. The heating power changes on-off in a stepwise fashion following the step function:

$$H(t) = \sum_{m=1}^{\infty} \frac{1}{2m-1} \sin((2m-1)\Omega t).$$

(Here notations are standard.) The evolution (e.g., electron temperature and density) is measured with high space-time resolution. Figure 3 (a) illustrates the radial profile of the density and the mean electron temperature, and the radial diagnostic position of the temperature is indicated. The fluctuation intensity was measured using a reflectometer at a few radial positions. The temporal evolutions (ECH power, stored energy, temperature, and fluctuation intensity) are illustrated in Fig. 3 (right).

The convolution method (the conditional average) was applied to the temporal data. The accumulation of experimental data by the conditional average (here, the time of the turning-off of the ECH power was chosen as the reference time) and the periodic response was deduced from the data. Figure 4 illustrates the period-averaged data of the periodic components in the heating power, density, electron temperature, its gradient, heat flux, and fluctuation intensity for various frequency bands.

The heat flux was evaluated according to the following procedure. Using the periodic time evolutions of T_e at various radial measurement points, we plotted the spatio-temporal evolution of the temperature response, as shown in Fig. 5. Figure 5 displays two time scales (shown by the white and black dashed lines) that will be discussed later. Using the data for $T_e(r, t)$, we evaluated the heat flux from the following relation:

$$\delta q_e(\rho, t) = -\frac{1}{S(\rho)} \int_0^{\rho} dV \left(\frac{3}{2} n_e \frac{\partial \delta T_e}{\partial t} - p_{ECH}(\rho, t) \right).$$

(1)

Note the time resolution of the measurement. The two terms in the parenthesis on the RHS usually have differ-
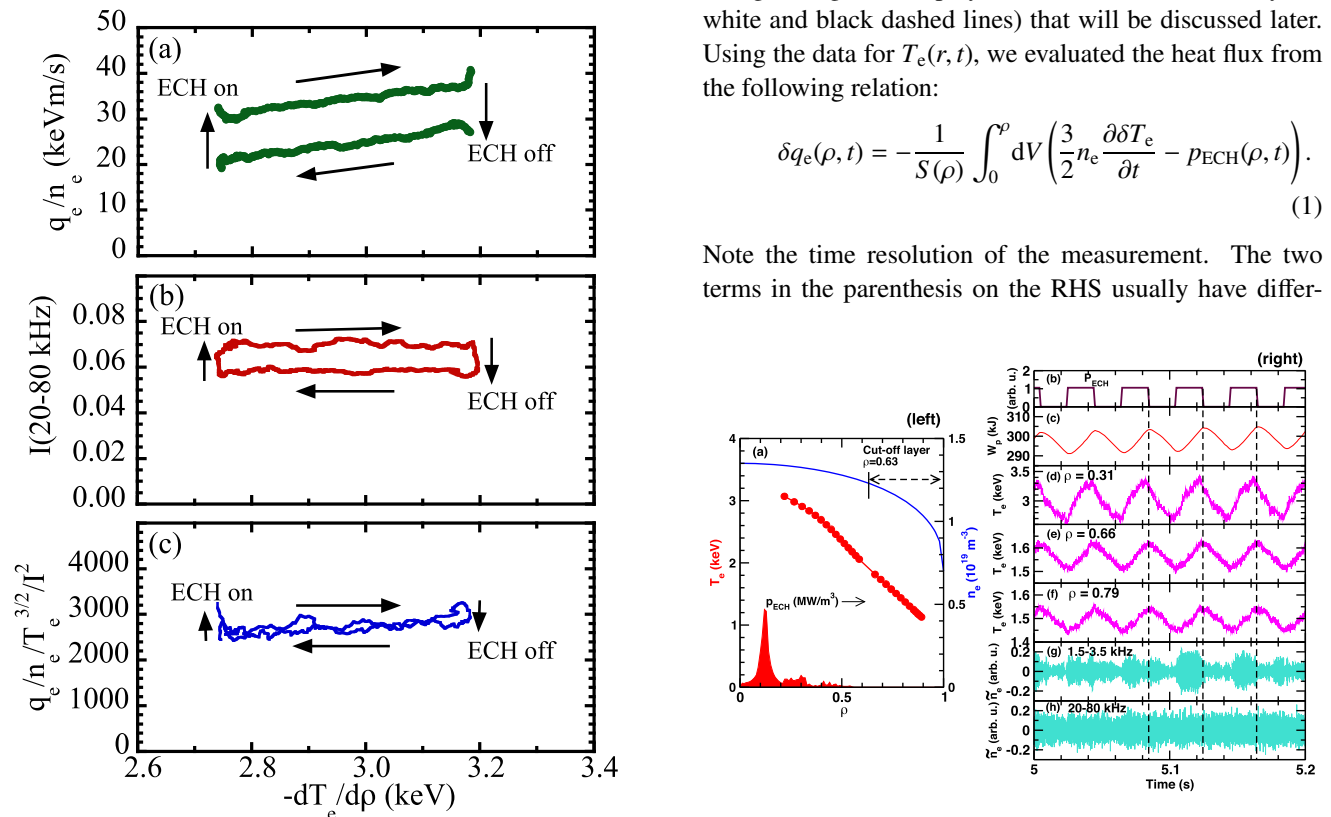

Fig. 2 Measurements from LHD: (a) the heat flux and (b) the fluctuation intensity as functions of gradient. Also shown is (c) the normalized heat flux. Reproduced from Ref. [7].

Fig. 3 The MECH experiment on the LHD: (left) the radial profiles and (right) the temporal evolution. The heating profile on the left is given by a ray-tracing calculation. Adopted from Ref. [3].
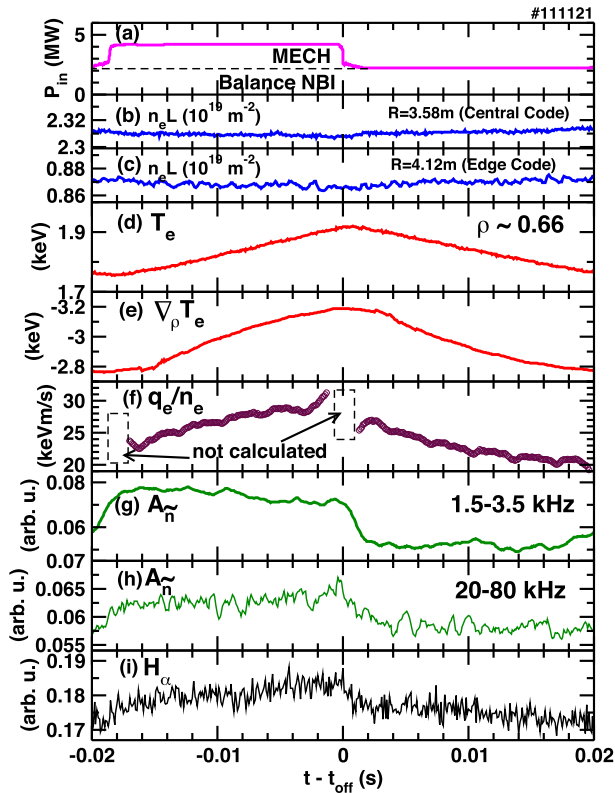
Fig. 4 Periodic responses owing to the MECH are deduced from the conditional average, where the reference time is chosen as the time "off". Reproduced from Ref. [3].
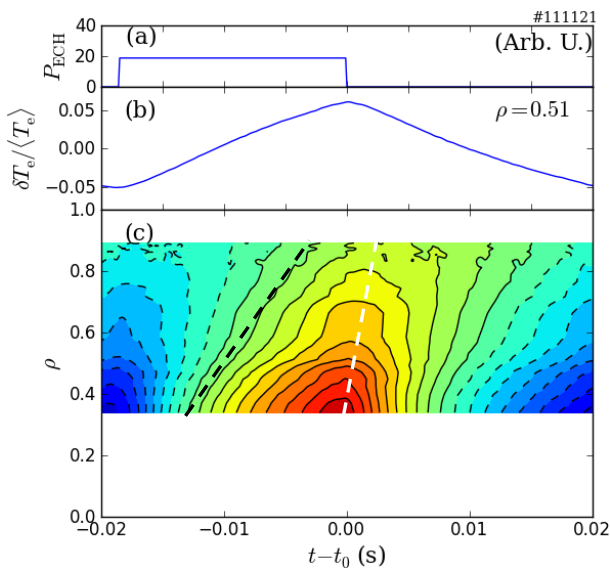

Fig. 5 The spatio-temporal evolution of the temperature response in the MECH. The reference time is chosen at the off-time of ECH. Two time scales of propagation (the black and white dashed lines) are seen. Reproduced from Ref. [6].

Fig. 6 Dependencies of (a) the conditional-averaged intensity of fluctuation in the frequency range 20 - 80 kHz and (b) the heat flux on ∇T_e. The fluctuation intensities are normalized by their average values for a period. Arrows denote the direction of the variation. Reproduced from Ref. [3].

signal-to-noise (S/N) of the diagnostic system of electron cyclotron emission (ECE). To eliminate an artificial temporal spike in the deduced heat pulse, where the surge in the flux is introduced by the difference in the time scales, a low-pass filter is applied to the signal of the heating power, $P_{ECH}(r, t)$. The cut-off frequency of the filter is adjusted to the high frequency limit (time resolution) of the $T_e(r, t)$ measurement. After this filter processing step, the modulated heat flux is calculated as in Fig. 4 (f). Figure 4 illustrates the simultaneous measurement of the temperature gradient (e) and the heat flux (f). Using Figs. 4 (e) and (f), the flux and fluctuation intensity can be drawn as functions of the gradient, as shown in Fig. 6.

The "abruptness" of the change in the heat flux when the heating power is switched on was evaluated to be O(1) ms or less. This is the upper bound imposed by the time resolution of the ECE diagnostics.

2.2 Fourier analysis method

We propose an additional experimental method to confirm the hysteresis. The evaluation of the heat flux demands a large number of ECE channels. Even if the channel number is limited, the hysteresis relation can be confirmed by observing the very-higher-order harmonics of a moduational ECH. Figure 5 indicates that there are two time-scales in the radial propagation of the change, which starts from the core. The first change at the on or off very rapidly propagates to the edge, while the gradual change propagates at much slower velocity. The presence of these two time-scales is the origin of the discrepancy between

ent time resolutions. The heating power is normally evaluated with very high time resolution, while the measurement of the rate of change of the temperature is limited by the
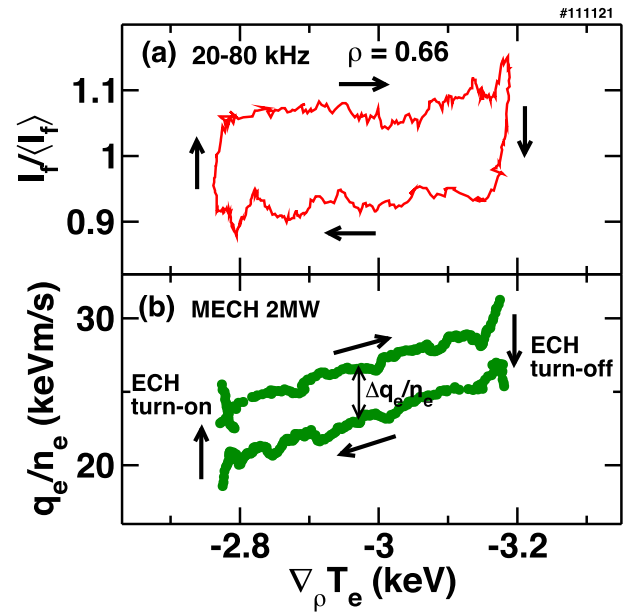
the power-balance and heat-pulse conductivities. Once we noticed that the simple local closure of the flux relation (the diffusion model) was broken, the discrepancy between these two "conductivities" was easily resolved (see, e.g., Ref. [8]).

This two-timescale property can be explicitly studied by observing the radial dependence of the amplitude of higher harmonics. If the heat flux follows the diffusive model including the pinch effect, then

$$q = -n\chi\nabla T. \tag{2}$$

The eigenfunction of the m-th harmonic of the temperature perturbation is

$$\delta T_m(x) \sim \exp\left(-\sqrt{m\omega_1/2\chi}\,x\right), \tag{3}$$

where ω_1 is the fundamental frequency of the modulation. That is, the amplitude of the higher order harmonics decay exponentially at large distances. By contrast, when hysteresis in the gradient-flux relation exists,

$$q = -\chi\nabla T + q_{\text{jump}}, \tag{4}$$

and the Fourier spectrum changes dramatically at higher harmonics. We can characterize the jump in the hysteresis by the parameter Q:

$$-\nabla \cdot q_{\text{jump}} = QH(t). \tag{5}$$

We here assume that Q is a weakly varying function in space. Then the transport equation,

$$\frac{\partial}{\partial t}T - \chi\nabla^2 T = QH(t),$$

gives the behavior of the perturbation at higher harmonics as

$$T_{2m-1} \sim \frac{-Q}{(2m-1)^2}\cos((2m-1)\Omega t). \tag{6}$$

Comparing the terms in Eq. (6) to those of Eq. (3), we see that the influence of the jump in the hysteresis is prominent in the higher harmonics [8]. First, while the diffusive model shows exponential decay in radius and harmonic number, the jump in hysteresis introduces a term that depends on the harmonic number m in an algebraic manner. The radial shape of the perturbation has a weak dependence on m. Therefore, by observing the higher harmonics, the presence of a jump in the hysteresis can be observed.

Using an advanced data analysis, such as conditional average, harmonics, such as the 7th, have been studied. This method was successfully applied to LHD and TJ-II [9, 10]. Observations of higher harmonics in the temperature fluctuation are shown in Fig. 7 (left). A large number of higher harmonics were detected from the observations using the convolution method. The power of the m-th harmonic behaves as

$$\sim m^{-4} \text{ (at large } m), \tag{7}$$

as predicted by Eq. (6). The radial profile of the amplitude is shown for the fundamental component and the higher
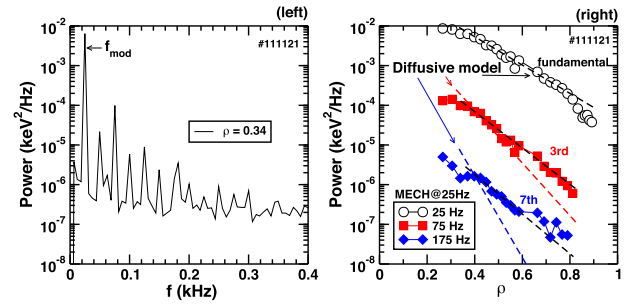

Fig. 7 Observations of the higher harmonics in heat wave propagation are shown to the left, and radial amplitude profiles of higher harmonics are shown to the right. It can be seen that the radial decay of higher harmonics is much slower than in the diffusion model (right: dashed lines). Reproduced from Ref. [9].
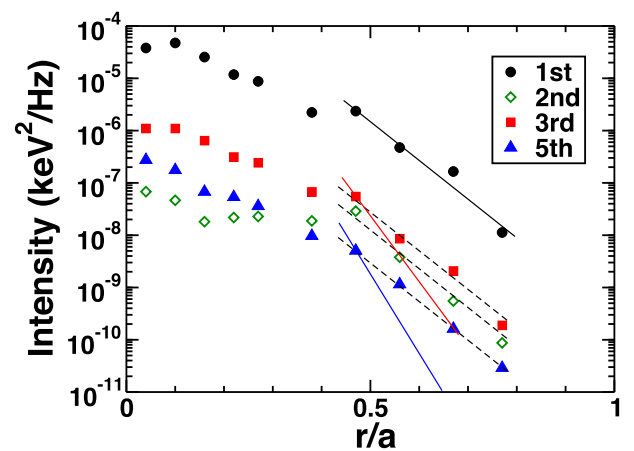

Fig. 8 The case of the TJ-II experiment. Radial profiles of the intensity of the fundamental, 2nd, 3rd, and 5th harmonics. Reproduced from Ref. [10].

harmonics Fig. 7 (right). In the figure, the dashed line indicates exponential decay, which is predicted by the diffusive model in which the effective diffusivity is fitted based on the estimation from the fundamental perturbation. It is clear that the radial decay of the higher harmonics is much slower than the diffusion model (dashed lines). If the "conductivity" is naively deduced following Eq. (3) and the radial profile of the higher harmonics (e.g., the 7th harmonic) is observed, this can result in an extremely large value of "conductivity". Notice that the radial dependences of the 3rd and 7th harmonics are similar to each other. The weak dependence of the radial profile of the higher harmonics indicates that the perturbed temperature propagates in radius while retaining its temporal shape.

The case of the TJ-II experiment is also shown in Fig. 8, including the radial profiles of the intensity of the fundamental, 2nd, 3rd, and 5th harmonics. Comparing the 3rd and 5th harmonics, a result similar to LHD is observed, which strongly suggests the presence of hysteresis in the gradient-flux relation.
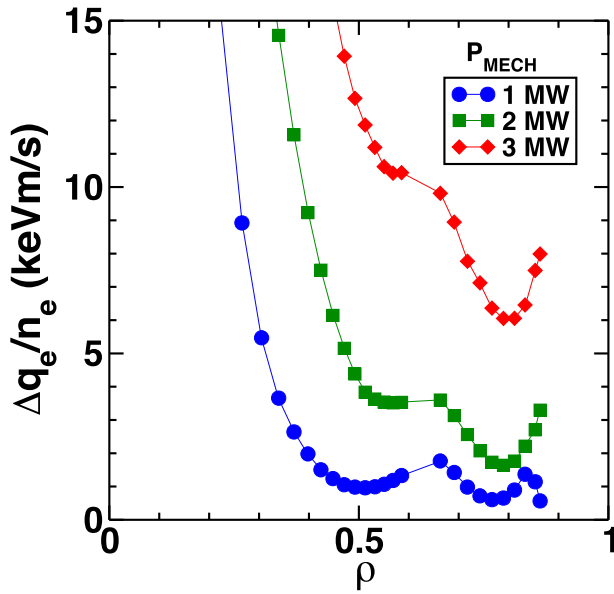
Fig. 9　Width of the hysteresis as a function of the radius for various modulation powers. The width of the hysteresis depends strongly on the modulation power. Reproduced from Ref. [3].

2.3　Parameter dependence of the hysteresis

　　The properties of this hysteresis have not yet been thoroughly studied. One clear fact is that the height of the hysteresis is an increasing function of the modulation power. Figure 9 indicates that the hysteresis height (at $r/a \sim 0.6$) grows more rapidly than the increment of the modulation amplitude (note that the base power is standard in this experiment). The "power degradation" of the global confinement, in the stationary state, is greatly influenced by the power dependence of the hysteresis.

3.　Theory

　　Motivated by the Stroth experiments, we examined whether the "nonlocal-in-space" interaction (e.g., the interaction via long-radial-wavelength fluctuations) can induce hysteresis in the gradient-flux relation [11]. If not, the direct effect of heating on the transport is not necessary. However, reports [3,6] show that "nonlocal-in-space" interactions are not sufficient.

　　To explain the process by which heating directly influences the turbulence, without waiting for changes in gradients and energetic particles, we examined the direct coupling of heating to turbulence in the kinetic equation [12]. The source, S, induces a fluctuation in the turbulent plasma:

$$S[f; \boldsymbol{x}, \boldsymbol{v}, t] = \bar{S}[f_0; \boldsymbol{x}, \boldsymbol{v}, t] + \frac{\delta S[f_0; \boldsymbol{x}, \boldsymbol{v}, t]}{\delta f_0}\tilde{f} + \cdots \tag{8}$$

This process is usually neglected; however, we should consider the process of "*heating by turbulence*". The new coupling coefficient that controls the direct influence of heat-
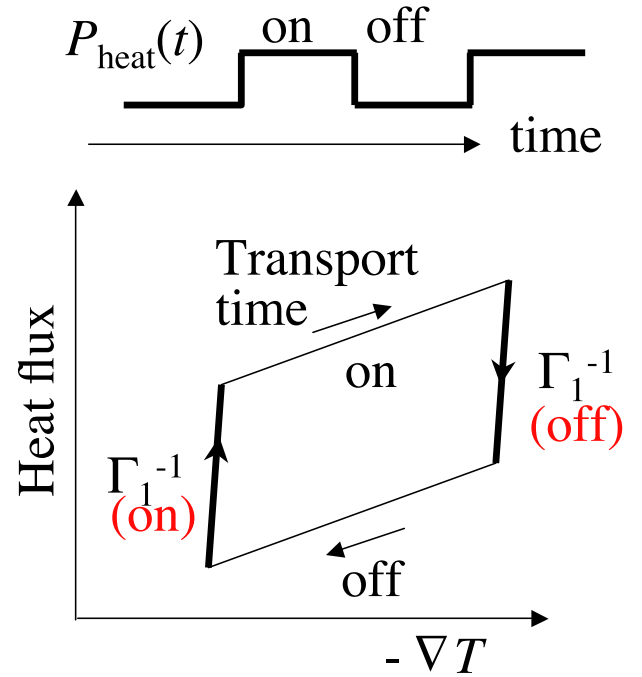

Fig. 10　The gradient-flux relation during periodic modulations of the heating power (theory).

ing on turbulence depends on the features of the source (e.g., electrons, ions, or momentum) [13, 14]. The dependence of the hysteresis height on the heating power has been discussed [12–15]. The fluctuation amplitude is influenced (enhanced) by the heating directly as

$$\langle \varphi_1 \varphi_1 \rangle = \frac{1}{1 - \gamma_h \chi_0^{-1} k_\perp^{-2}} \langle \varphi_1 \varphi_1 \rangle_0 \qquad \gamma_h \equiv \frac{\partial P}{\partial p}, \tag{9}$$

where the denominator includes the term γ_h, i.e., the direct influence of the source (the heating power). This term, γ_h, is proportional to the intensity of the source. Therefore, as the heating becomes stronger, the fluctuation intensity and turbulence-driven transport increases without changing the global plasma parameters.

　　This result, Eq. (9), explains the rapid change in the heat flux associated with the change in the heating. If the heating scheme is such that the heating absorption rate is an increasing function of the plasma pressure (such as radio frequency (RF) heating), γ_h is positive. In such a case, the turbulence and turbulent transport coefficient increase almost immediately within the nonlinear decorrelation time of the turbulence without waiting for a change in the gradients. Figure 10 illustrates the heat flux as a function of the gradient during the period modulation of the heating power. Equation (9) also indicates that, as the amplitude of the modulation in the heating power increases, the hysteresis height will increase faster than the amplitude of the modulation.

4. Future Research Topics

These studies indicate the necessity to reconstruct the gradient flux relation. The property of the newly assessed component in the energy flux (the jump in the hysteresis) must be thoroughly investigated. The jump in the hysteresis can depend on the relative relationship between the radius of the observation and that of the power absorption. Further, the circulation in the hysteresis loop is different (as illustrated in Fig. 1 (b)) depending on the location of the observation when the modulated power is absorbed at mid-radius [2]. Such a disparity in the response, between the inside and outside of the absorption domain, has also been noted in the dynamic response of edge plasmas [16]. An experiment of off-axis power modulation was performed on TORESUPRA. The analysis was performed based on a local transport model (which employs the thermal conductivity and pinch model) and the dynamics were interpreted in terms of the localized "pinch term" with a complex radial distribution [17]. The off-axis power modulation (at the mid-radius, $r/a \sim 1/2$) is currently being performed on HL-2A. An in-depth study will be possible by executing a modulation of the central heating to compare the cases of off-axis and central modulations. Further analysis, based on the advanced data analysis method, of various heating profiles will also be beneficial.

Another key issue concerns the responses of the particle and momentum fluxes at the onset of heating. Phenomenologically, the concept of the density pump by ECH has long been known. For recent analyses, see Refs. [18] and [19]. The rapid response of the particle flux at the onset of heating has been indicated in the case of the MECH experiment. The interrelationship between the particle and energy fluxes will be investigated in detail in future studies. Observations of the responses of plasma velocities have also been initiated [16], and the dynamic hysteresis loop in the velocities has been reported. A unification of studies on energy, particle, and momentum transport will be a central issue in future studies.

5. Summary

The existence of hysteresis in the gradient-flux relation (in the core plasma as well as at the edge) is now unambiguous. In this overview, we explained a method to identify the hysteresis in the gradient-flux relation in the core plasma using a modulational heating experiment. An introduction was made to the advanced data analysis method. Then, we explained the theoretical analysis of a process where the source couples directly to the fluctuations (a process linking heating and turbulence). The new picture of transport relations, which employs the hysteresis in the gradient-flux relation, will provide progress in understanding the confinement of toroidal plasmas.

Appendix. An Additional Discussion of the Telegraph Equation Model

While the telegraph equation can reproduce fast propagation dynamics in various problems, this model does not adequately explain the observation of transport hysteresis. The telegraph equation model explains the fast propagation of change; however, the phase relationship between the temperature gradient and the heat flux is opposite to that in experimental observations [20].

The comparison is explained as follows. The telegraph equation includes a finite relaxation time for the turbulence intensity in response to the changes in the global plasma parameters. The delay time τ is introduced as follows.

$$\frac{3}{2}n\frac{\partial \tilde{T}}{\partial t} = -\nabla \cdot \tilde{q} + \tilde{p},$$

$$\frac{\partial \tilde{q}}{\partial t} = -\frac{\tilde{q} - \tilde{q}_0}{\tau}, \qquad \tilde{q}_o = -n\chi\nabla\tilde{T}. \qquad (A1)$$

Combining these relations, one forms the telegraph equation,

$$\frac{\partial^2 \tilde{T}}{\partial t^2} + \frac{1}{\tau}\frac{\partial \tilde{T}}{\partial t} - \frac{2\chi}{3\tau}\nabla^2\tilde{T} = 0, \qquad (A2)$$

where n and χ are assumed to be constant. Equation (A2) is a generalization of the conventional diffusion equation. In the limit of short relaxation times, $\tau \sim 0$, the diffusion equation is recovered. In the limit of τ longer than the oscillation period, the second term in Eq. (A2) becomes negligible, and Eq. (A2) approaches the wave equation without dispersion.

This model was applied to non-diffusive radial heat pulse propagation under periodic modulation of the heating power. The model showed some success in reproducing the amplitudes of the higher harmonics. That is, as is shown in Fig. A1 (a), the decay of the higher harmonics is much weaker than in the diffusive model. This indicates that the information for the change propagates much faster to the edge than in the diffusive model. However, the phase relation between the temperature gradient and the heat flux is opposite to that in the experimental observations, as shown in Fig. A1 (b).
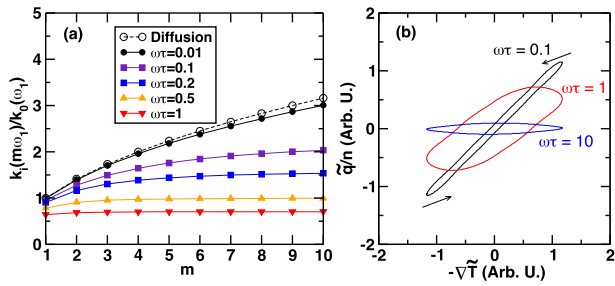
Fig. A1 The prediction of the telegraph equation model. We see in (a) that the decay of higher harmonics is much weaker in this model; however, in (b) the change in the gradient-flux relation is opposite to that in the experiment.

[1] U. Stroth, L. Giannone, H.-J. Hartfuss, the ECH Group and the W7-AS Team, Plasma Phys. Control. Fusion **38**, 611 (1996).

[2] K.W. Gentle, M.E. Austin, J.C. DeBoo, T.C. Luce and C.C. Petty, Phys. Plasmas **13**, 012311 (2006).

[3] S. Inagaki *et al.*, Nucl. Fusion **53**, 113006 (2013).

[4] N.J. Lopes Cardozo, Plasma Phys. Control. Fusion **37**, 799 (1995).

[5] F. Ryter *et al.*, Phys. Rev. Lett. **86**, 5498 (2001).

[6] S. Inagaki *et al.*, Plasma Fusion Res. **8**, 1202172 (2013).

[7] K. Ida, Z. Shi, H.J. Sun, S. Inagaki, K. Kamiya, J.E. Rice, N. Tamura, P.H. Diamond, G. Dif-Pradalier, X.L. Zou, K. Itoh, S. Sugita, O.D. Gurcan, T. Estrada, C. Hidalgo, T.S. Hahm, A. Field, X.T. Ding, Y. Sakamoto, S. Oldenbuerger, M. Yoshinuma, T. Kobayashi, M. Jiang, S.H. Hahn, Y.M. Jeon, S.H. Hong, Y. Kosuga, J. Dong and S.-I. Itoh, Nucl. Fusion **55**, 013022 (2015).

[8] K. Itoh *et al.*, J. Phys. Soc. Jpn **85**, 014501 (2016).

[9] S. Inagaki *et al.*, Plasma Fusion Res. **8**, 1202173 (2013).

[10] S. Inagaki *et al.*, Plasma Fusion Res. **9**, 1202052 (2014).

[11] T. Iwasaki, S.-I. Itoh, M. Yagi, K. Itoh and U. Stroth, J. Phys. Soc. Jpn. **68**, 478 (1999).

[12] S.-I. Itoh and K. Itoh, Sci. Rep. **2**, 860 (2012).

[13] S.-I. Itoh and K. Itoh, Nucl. Fusion **53**, 073035 (2013).

[14] Y. Kosuga, S.-I. Itoh and K. Itoh, JPS Conf. Proc. **1**, 015002 (2014).

[15] K. Itoh and S.-I. Itoh, Plasma Fusion Res. **10**, 027 (2015).

[16] K. Kamiya *et al.*, Observation of the inward propagation of spontaneous toroidal flow from the plasma boundary in the Large Helicon Device, submitted to Phys. Rev. Lett. (2015).

[17] S.D. Song *et al.*, Nucl. Fusion **52**, 033006 (2012).

[18] S. Kubo *et al.*, Plasma Fusion Res. **3**, S1028 (2008).

[19] R. Makino *et al.*, Plasma Fusion Res. **8**, 2402115 (2013).

[20] S. Inagaki, Plasma Fusion Res. **10**, 1203002 (2015).